Structure of a liquid–vapor interface in the presence of a hard wall in the transition region

M. Rao and B. J. Berne[a)]

Department of Chemistry, Columbia University, New York, New York 10027

J. K. Percus and M. H. Kalos[b)]

Courant Institute of Mathematical Sciences, New York University, New York 10012
(Received 8 May 1979; accepted 9 July 1979)

The structure of a liquid–vapor interface, in the presence of a hard wall in the transition region, is studied using Monte Carlo simulation. Both longitudinal and transverse correlations are compared to those observed in a free interface. The density profile shows a transition from an oscillatory profile to a smooth monotonic one when the position of the hard wall is varied. It is shown that these results are consistent with a heuristic capillary wave theory of the interface.

I. INTRODUCTION

The structure of the planar gas–liquid interface has received much attention in recent years.[1–6] The interface can be characterized by several parameters. Let $z_0(x, y)$ specify the instantaneous height of the interface above a point (x, y) in a reference plane parallel to the interface, and let $\Delta z(x, y)$ specify the intrinsic thickness of the interface at (x, y). The picture that seems to be emerging is that Δz is less than the intermolecular spacing in the liquid phase near the triple point, and that $z_0(x, y)$ varies considerably as a function of (x, y). The instantaneous structure is analogous to that of a vibrationally excited membrane or drumhead with some intrinsic thickness. The thermally excited waves—capillary waves—arise and decay like any thermal fluctuations in the liquid phase. The observed relatively broad transition density profile is then the average of an ensemble of gas–liquid boundaries in the form of thermally excited capillary waves. If this picture is valid, it should also apply when the observed profile is intentionally distorted.

When a hard repulsive wall is in the vapor, located far from the interface, it should not influence the density profile.[3] However, when the wall is located in the interfacial transition region, it must perturb the density profile, presumably damping the capillary waves. The response of the interfacial and bulk structure to the wall should then provide important information about the various approximations used in the theory of the interface. In this paper, we will show that the response does maintain consistency with the broad picture of a surface shaped by excitation of capillary waves.

When a repulsive wall is positioned in the transition zone, the two phase coexistence line $P(T)$ will depend upon the reduced available surface thickness, resulting in a new class of interfacial thermodynamics. We initiate the study of this thermodynamics.

[a)]Supported by grants to B. J. Berne from the National Science Foundation (NSF CHE 76-11002) and the National Institutes of Health (NIH-R01 NS 12714-03).

[b)]Supported by the Department of Energy under contract EY-76-C-02-3077*000.

II. THE SYSTEM STUDIED

Here we report the results of a Monte Carlo simulation of a system containing 1728 classical particles interacting via a truncated and shifted Lennard-Jones (12-6) potential with "core diameter" σ:

$$\phi(r) = V(r) - V(r_0) ,$$

$$V(r) = \begin{cases} 4\epsilon\left[\left(\frac{\sigma}{r}\right)^{12} - \left(\frac{\sigma}{r}\right)^{6}\right], & r \le r_0 , \\ 0 , & r > r_0 . \end{cases}$$

The cutoff radius r_0 is 2.5σ, the reduced temperature kT/ϵ is set to 0.7, slightly above the triple point temperature, and the system is placed in a box with the two square faces of dimension $L = 13.15\sigma$ and constrained to be periodic in those directions. It is the third dimension of the box that will be controlled in this study.

Much is already known about similar systems. Several years ago, Rao and Levesque[7] and Kalos, Percus, and Rao[8] studied the interfacial profile, the transverse structure factor, and the surface tension of a sheet of this liquid in equilibrium with vapor at the same temperature. They first equilibrated a homogeneous fluid using a rectangular cell of area $L \times L$ in the x–y plane and length M along z direction. The primary cell was then removed and placed in the center of a rectangular box of cross-sectional area $L \times L$ but of thickness M surrounded by a vacuum of thickness M on both sides. Subsequent simulation led to evaporation and finally to sheets in equilibrium with vapor.

The specific geometry established is important from the viewpoint of maintenance of a planar interface. In free space, without imposed gravity, a volume of liquid will ultimately take on the minimum surface/volume shape of a sphere, to within fluctuations and curvature effects. In a domain with two periodic directions, only two of the six surfaces which would usually bound a rectangular box will appear as free boundaries. Hence, a planar sheet of thickness h will still be stable against spherical droplet formation if its volume to surface ratio exceeds that of a sphere: $L^2h/2L > (L^2h/36\pi)^{1/3}$, or $h > (2/9\pi)^{1/2}L \sim 0.27L$. Hence, the sheet studied in Refs. 7 and 8 (with $h = 14\sigma$, $L = 13.15\sigma$) is stable.

 0021-9606/79/213802-05$01.00

TABLE II. Table showing the pressure, wall density, liquid density, and average density as a function of the wall position.[a]

z_p	Location of the wall z_w	Pressure p	Wall density n_w	Liquid density n_l	Average density $\bar{n}$	Gibbs surface z_G
6.1	6.6	0.65	0.94	0.85	0.76	5.89
6.57	7.06	0.29	0.33	0.80	0.71	6.25
···	Free interface	$p_\infty = 0.002$	$n_\infty = 0.0033$	0.77	···	6.5

[a]Reduced units are used.

III. SURFACE LAYER THERMODYNAMICS

The present study differs from those cited above in one technical way and one conceptual way. Technically, since we are investigating the state of thermal equilibrium, we choose to use a Monte Carlo simulation instead of molecular dynamics. The ordinary Metropolis scheme is used with a step size of 0.1σ. Conceptually, our objective is to alter the state of the surface layer. This we do by introducing hard walls at z_w on both sides of the rectangular liquid slab (centered at $z=0$) in the sense that all particles must have their centers located within $|z| \le z_p \equiv z_w - \frac{1}{2}\sigma$. In particular, the values $z_w = 20\sigma$, 7.07σ, and 6.6σ have been chosen—the first being far out in the very low density ($n \sim 0.003$) gas region, and the latter two within the interfacial region of the free interface.

In Table I, we report the thermodynamic parameters resulting from varying the wall placement. We list the position of the wall z_w, the virial-derived hydrostatic pressure P, and the wall density $n_w = n(z_p)$, as well as the liquid density n_l and the average density $\bar{n} = N/2L^2 z_w$. As a consistency check, it can be seen that the data are in reasonable agreement with the exact theoretical result[9]

$$P = n_w kT \ . \tag{2}$$

In addition, the "Gibbs surface" location z_G is determined. z_G is the position at which a slab of uniform liquid density (surrounded by nominally 0-density gas) would contain all of the particles of the system. Clearly, $z_G = 1728/2n_l L^2 = 5/n_l$. Our data do not go nearly as far as insertion of a wall into bulk liquid. In that case, one would expect a net pileup of particles near the wall, resulting in $z_G > z_p$, a condition which is far from being obtained in our simulations so far.

How well do our data accord with the general picture of a surface composed of capillary wave excitations? If there is an intrinsic density profile $n_0(z)$ for $0 \le z \le z_0$ (regarding gas density as 0), and a free surface capillary wave amplitude distribution $f(z)$ on the intrinsic constrained surface $z = z_0$, the resulting density will of course be

$$n(z) = \int f(\xi)\, n_0(z-\xi)\, d\xi \ , \tag{3}$$

where $\xi = z - z_0$.

Previous work[8] suggests a normal distribution of capillary wave amplitudes

$$f(\xi) = 1/\Delta\sqrt{2\pi}\, e^{-\xi^2/2\Delta^2} \ , \tag{4}$$

where $\Delta \sim 0.9$ for the present system. Now, if a wall is inserted at z_c, the primary effect should be that ξ is bounded by $a \equiv z_c - z_0$ and

$$f_a(\xi) = f(\xi)\, \theta(a-\xi) \Big/ \int_{-\infty}^{a} f(\xi')\, d\xi' \ , \tag{5}$$

where $\theta(x)$ is the unit step function. In addition, one can imagine a general rise in bulk density n_l to accord with the reduced volume. The intrinsic profile, with a fraction of particles necessarily at $z = z_0$, should have the form $n_0(z) = n_0\, \delta(z - z_0) + n_1(z)$, where $n_1(z)$ is nonsingular. An immediate consequence is that, at the wall $z = z_0 + a$, where only the edge of the intrinsic $n_0(z)$ contributes,

$$n_w = \beta P = n_0 f(a) \Big/ \int_{-\infty}^{a} f(\xi')\, d\xi' \ . \tag{6}$$

The pressure data in Table I are closely reproduced by assuming $n_0 = 1$, $z_0 = 5.8$ (with $a = 0.8$ and 0.3 for the two wall positions), which are reasonable assessments of the intrinsic profile. This approach along with the ensuing arguments provides a heuristic rather than a rigorous picture of the liquid vapor interface in the presence of a hard wall.[10]

IV. MICROSCOPIC DENSITY

Figure 1 shows how the density profile is perturbed by the walls. In the two significant cases, the walls are located in the interfacial region. A pair of walls placed at $z_w = 7.07$ simply truncates the profile and compresses the liquid. However, a small displacement ($z_w = 6.6$) of the walls towards the liquid leads to a

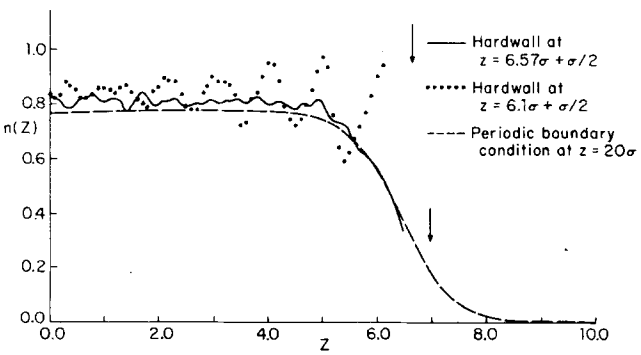

FIG. 1. The symmetrized density profile $n(z)$ as a function of z. (a) The dashed lines show the free interface (taken from Ref. 8). (b) The full line shows the density profile when walls are located at $\pm 7.07\sigma$. (c) The dots show the density profile when the walls are located at $\pm 6.6\sigma$.

dramatic response characterized by an oscillatory density profile (dotted curve in Fig. 1). This qualitative change is associated with a wall density n_w lower than the bulk density n_1 in the first case, rising to $n_w > n_1$ in the second case. Could it be that oscillations set in only when $n_w > n_1$? Of course, the extremes are clear enough. Oscillations are to be expected for a compressed liquid, and represent correlation effects. When the wall is further out into vapor, the density profile, although truncated, still follows the free interfacial profile very closely. However, the first regime should go continuously into the second, and we surmise that, even when the pressure is larger than vapor pressure, the system should be regarded as consisting of two phases—a bulk and a surface phase.

These qualitative effects are certainly explicable in terms of a capillary wave theory even of the primitive type described above. As we have mentioned, the existence of capillary waves means that, viewed from a transverse location $(x, y) = \mathbf{x}$, a planar intrinsic surface extending laterally over a coherence length sweeps back and forth with a distribution $f(\xi)$ for its z location. This gives rise to Eq. (3). If the primary effect of a wall is to truncate $f(\xi)$, as in Eq. (5), we then have

$$n(z) = \int_{-\infty}^{a} f(\xi)\, n_0(z-\xi)\, d\xi \Big/ \int_{-\infty}^{a} f(\xi)\, d\xi \ . \tag{7}$$

The intrinsic profile $n_0(z)$ is, loosely speaking, the conditional distribution that a particle be at z when it is known that the surface is at z_0. The oscillation wavelength of n_0, i.e., λ, should resemble that of the pair correlation function g. It appears that $\lambda \sim 1$, and so the oscillations due to the intrinsic profile will be smoothed away by a Gaussian with width $\Delta \sim 0.9$. Thus, in the absence of the wall, there will be no oscillations in $n(z)$. When, however, a wall is introduced, it truncates the wing of the Gaussian at a. When $a = 0.8$, the wall does not truncate the Gaussian profile very much and the oscillations are still wiped out. When the wall is pushed to $a = 0.3$, about half the Gaussian is gone, narrowing the standard deviation to ~ 0.5. Now, $f_a(\xi)$ is sufficiently narrow that it can resolve the $\lambda \sim 1$ wave in the pair correlation function, which it does.

V. TRANSVERSE CORRELATIONS

Pertinent to the study of how the wall damps the capillary waves is the behavior of the transverse structure factor $S(k, z)$ for the wavelength $k = (2\pi/L)(m_x^2 + m_y^2)^{1/2}$ allowed for by periodicity in the x, y plane. This function is by definition

$$S(k, z) = \frac{\langle \sum'_{ij} e^{i\mathbf{k}\cdot(\mathbf{r}_i - \mathbf{r}_j)} \rangle}{\langle \sum'_{ij} 1 \rangle} \ ,$$

where the prime indicates that we sum over all particles i and j that are in a layer between $z - \frac{1}{2}\Delta z$ and $z + \frac{1}{2}\Delta z$, and k is in the xy plane. Although Δz was taken as 0.1σ for the determination of the density profile, reasonable statistical accuracy requires us to take it as 0.8σ for $S(k, z)$. The transverse structure factor is shown in Figs. 2(a), 2(b), and 2(c), respectively, for the free interface, the wall at $z_w = 7.07\sigma$, and the wall at 6.6σ.

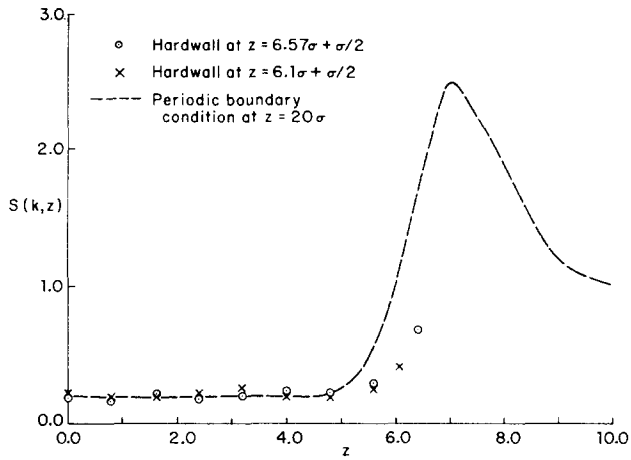

FIG. 2. The symmetrized transverse structure factor $S(k, z)$ as a function of z for smallest wave vector $k = 2\pi/L$. (a) The dashed lines show $s(k_1 z)$ for a free interface (taken from Ref. 8). (b) The circles show $S(k, z)$ when the walls are situated at $\pm 7.07\sigma$. (c) The crosses $S(k_1 z)$ when the walls are situated at $\pm 6.6\sigma$.

$S(k, z)$ can be interpreted as an isothermal compressibility. It is discussed more fully in Ref. 8, where it is shown that, for a free interface, $S(k, z)$ goes as $1/k^2$ for $k \to 0$ in the interfacial region. This indicates very long range correlations in density in the xy plane.[11] The analysis of Ref. 8 is readily extended to the imposition of a wall at z_p (see Appendix A) and yields an expression of the form

$$S(k, z) = \frac{n'(z) n'(z)}{[c(z_p, z_p)\, n_w^2 + \beta\gamma k^2]} + \text{terms weakly dependent on } k \text{ and } z \ , \tag{9}$$

where γ is the surface tension. Thus, the capillary wave induced $1/k^2$ dependence at low k is quenched by the wall with n_w^2 as the dominant parameter, an effect that is seen at least qualitatively in Figs. 2(b) and 2(c). In Fig. 2, we have chosen to plot

$$S(k, z) = \int_{\Delta z} \int_{\Delta z} S(z, z'; k)\, dz\, dz' / [n(z)\, \Delta z]^2 \tag{10}$$

and used only the minimum value $k_0 = 2\pi/L$, since the statistics are poorer at higher values.

VI. THE DAMPING MECHANISM

The formula (9) does not indicate the physical effect responsible for damping the transverse correlations in the presence of a wall. It is directly attributable to the capillary wave propagation. Since the analysis is complicated by the singularity of the wall potential, we shall here simply indicate how a smooth external potential changes the amplitude of the capillary waves and correspondingly the smearing of the surface-induced correlations.

We again consider[8] a capillary distortion $\xi(\mathbf{x})$ of the intrinsic profile $n_0(z)$, ξ now depending upon lateral location $\mathbf{x}$; on the average, then

$$n(z) = \langle n_0[z - \xi(\mathbf{x})] \rangle$$
$$= \frac{1}{2\pi} \int \tilde{n}_0(s)\, e^{-is\xi} \langle e^{is\xi(\mathbf{x})} \rangle\, ds \ , \tag{11}$$

where $\tilde{n}_0(s)$ is the Fourier transform of $n_0(z)$. The energy associated with the capillary wave is

$$\Delta E = \gamma \int [1 + |\nabla \xi(x)|^2]^{1/2}\, d^2x + \int n_0[z - \xi(\mathbf{x})] u(z)\, d^3r \ , \tag{12}$$

where γ is the surface tension and $u(z)$ the applied external potential field. If we expand to second order in ξ and, in treating long-range correlations, assume that

$$n_{2\,0}(\mathbf{x}, z, \mathbf{x}', z') = n_0(z)\, n_0(z') \ , \tag{13}$$

then it can be shown (see Appendix B) that

$$S(z, z', k) = \frac{n'(z)\, n'(z')}{\beta\gamma k^2 + \int n_0''(z) \beta u(z)\, dz} + \cdots \ , \tag{14}$$

precisely of the form (9). In terms of the external force field $F(z) = -u'(z)$, then $\int n_0'(z) \beta u(z)\, dz = -\int n_0'(z) \beta F(z)\, dz$ induces a positive damping if the force comes into the liquid from the gas, as expected. Equation (14) shows explicitly the way in which the external force interacts with the free capillary waves to change the amplitude distribution of the capillary waves and consequently the density profile.

VII. CONCLUSION

There has been considerable theoretical effort devoted to understanding the structure of fluids near a hard wall.[1–8] The structure of the fluid near the wall is very sensitive to the attractive forces in the fluid whereas the bulk pair correlation function is remarkably insensitive to these attractive forces. It has often been suggested that the differences here and in the normal gas–liquid interface are primarily due to the energetics of capillary wave excitation. In this study, we have spanned the domain between free interface and strict wall boundary, and have shown that focusing on capillary wave excitations leads to a semiquantitatively consistent picture. More importantly, however, our study of the density profile near a hard wall should provide a severe test of microscopic theory of the liquid state. It is in this spirit that we offer our results.

APPENDIX A

In this Appendix, we sketch the derivation of Eq. (9) in Sec. V. The analysis follows closely that given in Ref. 8. We first recall the relation

$$-\beta \nabla u(r) = \int c^{(2)}(\mathbf{r}, \mathbf{r}') \nabla n(\mathbf{r}')\, d^3r' \tag{A1}$$

between an applied potential $u(\mathbf{r})$ and the resulting density $n(\mathbf{r})$. Here, $c^{(2)}$ is the linear response function

$$c^{(2)}(\mathbf{r}, \mathbf{r}') = -\delta \beta u(\mathbf{r}) / \delta n(\mathbf{r}')$$
$$= \delta(\mathbf{r} - \mathbf{r}')/n(\mathbf{r}) - c(\mathbf{r}, \mathbf{r}') \ , \tag{A2}$$

where $c(\mathbf{r}, \mathbf{r}')$ is the usual Ornstein–Zernicke direct correlation. Our measurements are concerned with the transverse Fourier transform

$$c(z, z'; k) = \int c^{(2)}(\mathbf{x}, z, \mathbf{x}', z')\, e^{i\mathbf{k}\cdot(\mathbf{x}-\mathbf{x}')}\, d^2x \tag{A3}$$

and the analogous transform $S(z, z'; k)$ of the structure function

$$S^{(2)}(\mathbf{r}, \mathbf{r}') = n(\mathbf{r}) n(\mathbf{r}') [g(\mathbf{r}, \mathbf{r}') - 1] + n(\mathbf{r}) \delta(\mathbf{r} - \mathbf{r}') \ . \tag{A4}$$

If n and u are strictly z dependent, Eq. (A1) transcribes to

$$-\beta u'(z) = \int c(z, z'; 0) n'(z')\, dz' \ . \tag{A5}$$

In the present case, u represents a wall for $z \geq z_p$. Let us restrict all variables to $z < z_p$, so that $u = 0$ in Eq. (A5) but the surface discontinuity in density must be included:

$$0 = \int c(z, z'; 0) n'(z')\, dz' + c(z, z_p)\, n_w \ . \tag{A6}$$

Thus, for small n_w, the eigenvalue of $c(z, z', 0)$ is very nearly zero with eigenfunction $n'(z)$. This will also be the case at low k, in which case $c(z, z', k)$ can be expanded as

$$c(z, z', k) = c(z, z', 0) + k^2 c'(z, z') + \cdots \ , \tag{A7}$$

where

$$c'(z, z') = \frac{1}{4} \int c^{(2)}(\mathbf{x}, z, \mathbf{x}', z') |\mathbf{x} - \mathbf{x}'|^2\, d^2x \ . \tag{A8}$$

Now, S is the matrix inverse of c:

$$\int S(z, z'; k) c(z', z''; k)\, dz'' = \delta(z - z') \ . \tag{A9}$$

It is dominated for small n_w and k by the small diagonal matrix element c_{00} of c with respect to its near eigenvector

$$\phi(z) \equiv \eta n'(z) \ . \tag{A10}$$

η is a normalization factor. Then,

$$c_{00}(k) = \eta^2 \int c(z, z'; k) n'(z) n'(z')\, dz\, dz'$$
$$= \eta^2 \left[c(z_p, z_p) n_w^2 + k^2 \int c(z, z') n'(z) n'(z')\, dz\, dz' + \cdots \right] . \tag{A11}$$

Hence, S is dominated by

$$S(z, z'; k) = S_{00}(k) \phi(z) \phi(z') + \cdots$$
$$= \phi(z) \phi(z') / c_{00}(k) + \cdots$$
$$= n'(z) n'(z') / [c(z_p, z_p) n_w^2 + \beta\gamma k^2] \ , \tag{A12}$$

where the familiar Triezenberg–Zwanzig[12] formula for surface tension γ in terms of c' has been used.

It is important to note that n_w in the computer simulations is not small. The analysis of the experiments based on the foregoing set of equations should thus be regarded as suggestive and not rigorous.

APPENDIX B

Equation (12) may be expanded to second order in the displacement $\xi(\mathbf{x})$ to yield the following relative Boltzmann factor:

$$\rho(\xi) = \exp\left[-\frac{1}{2}\beta\gamma\int(\nabla\xi)^2 d^2x + \beta\int n_0'(z)u(z)\,dz\int\xi(\mathbf{x})\,d^2x - \tfrac{1}{2}\beta\int n_0''(z)u(z)\,dz\int\xi(\mathbf{x})^2\,d^2x\right]. \tag{B1}$$

To maintain the location of the mean surface, we assume that $\int n_0'(z)u(z)\,dz = 0$. We then go over to the Fourier transform

$$\xi(\mathbf{x}) = \frac{1}{L^2}\sum_{\mathbf{k}}\xi_{\mathbf{k}}e^{-i\mathbf{k}\cdot\mathbf{x}}. \tag{B2}$$

Introduce

$$\begin{aligned}\xi_{\mathbf{k}} &= (\eta_{\mathbf{k}} + i\eta_{-\mathbf{k}})/\sqrt{2},\\ \xi_{-\mathbf{k}} &= (\eta_{\mathbf{k}} - i\eta_{-\mathbf{k}})/\sqrt{2},\\ \xi_0 &= \eta_0,\end{aligned} \tag{B3}$$

so that

$$\rho(\eta) = \exp\left\{-(\beta 2L^2)\sum_{\mathbf{k}}\left[\gamma k^2 + \int n_0''(z)u(z)\,dz\right]\eta_{\mathbf{k}}^2\right\}. \tag{B4}$$

Thus, the kth wave is damped by the factor

$$\frac{\gamma k^2}{\left[\gamma k^2 + \int n_0'(z)u(z)\,dz\right]}. \tag{B5}$$

We can now complete the density profile computation.

According to Eq. (B5), we now have

$$\langle e^{is\xi(\mathbf{x})}\rangle = \left\langle \exp[i(s\sqrt{2}/L^2]\sum_{\mathbf{k}\geq 0}(\eta_{\mathbf{k}}\cos\mathbf{k}\cdot\mathbf{x} + \eta_{-\mathbf{k}}\sin\mathbf{k}\cdot\mathbf{x})\right\rangle$$

$$= \exp-\left\{(-s^2/2\beta)\sum_{\mathbf{k}}\left[\gamma k^2 + \int n_0''(z)u(z)\,dz\right]^{-1}\right\}. \tag{B6}$$

It then follows that

$$n(z) = \int n_0(z-z')\,e^{-z'^2/2\sigma^2}\,dz', \tag{B7}$$

where

$$\sigma^2 = \frac{1}{\beta}\sum_{k}\left[\gamma k^2 + \int n_0'(z)u(z)\,dz\right]^{-1}.$$

The sum on k must be truncated at about an interparticle wave number. We observe that, at this level, only the potential strength $\int n_0'(z)u(z)\,dz$ enters.

Proceeding to pair correlations, we restrict our attention to long range, beyond the intrinsic correlation length, so that we can write

$$n_{20}(\mathbf{x}, z, \mathbf{x}', z') = n_0(z)\,n_0(z'). \tag{B8}$$

Hence,

$$\begin{aligned}n_2(\mathbf{x}, z, \mathbf{x}', z') &= \langle n_0[z - \xi(\mathbf{x})]n_0[z' - \xi(x')]\rangle\\ &= \frac{1}{(2\pi)^2}\int\int\tilde{n}_0(s)\tilde{n}_0(t)\,e^{-i(sz+tz')}\\ &\quad\times\langle\exp[is\xi(\mathbf{x}) + it\xi(\mathbf{x}')]\rangle\,ds\,dt,\end{aligned} \tag{B9}$$

but, from Eq. (16),

$$\begin{aligned}\langle\exp[is\,\xi(x) + it\xi(x')]\rangle &= \left\langle\exp\left[(i\sqrt{2}/L^2)\sum_{\mathbf{k}\geq 0}\eta_{\mathbf{k}}(s\cos\mathbf{k}\cdot\mathbf{x} + t\cos\mathbf{k}\cdot\mathbf{x}') + \eta_{-\mathbf{k}}(s\sin\mathbf{k}\cdot\mathbf{x} + t\sin\mathbf{k}\cdot\mathbf{x}')\right]\right\rangle\\ &= \exp-(1/2\beta)\sum_{\mathbf{k}}\left[s^2 + t^2 + 2st\cos k(\mathbf{x} - \mathbf{x}')\right]\left[\gamma k^2 + \int n_0''(z)u(z)\,dz\right]^{-1}\\ &= \exp[-(\sigma^2/2\beta)(s^2 + t^2)]\left[\left(1 - \frac{st}{\beta}\sum\cos\mathbf{k}(\mathbf{x} - \mathbf{x}')\right)\right]\left[\gamma k^2 + \int n_0''(z)u(z)\,dz + \cdots\right]^{-1}.\end{aligned} \tag{B10}$$

We conclude that

$$S(z, z', k) = \frac{n'(z)n'(z')}{\beta\gamma k^2 + \int n_0''(z)\beta u(z)\,dz} + \cdots, \tag{B11}$$

which is Eq. (14).

[1] D. Henderson, F. F. Abraham, and J. A. Barker, Mol. Phys. **31**, 1291 (1976).
[2] J. K. Percus, J. Stat. Phys. **15**, 423 (1976).
[3] E. Weisman, D. Henderson, and J. L. Lebowitz, Mol. Phys. **32**, 1373 (1976).
[4] D. E. Sullivan and G. Stell, J. Chem. Phys. **67**, 2567 (1977).
[5] W. F. Saam and C. Ebner, Phys. Rev. A **17**, 1768 (1978).
[6] F. F. Abraham, J. Chem. Phys. **68**, 3713 (1978).
[7] M. Rao and D. Levesque, J. Chem. Phys. **65**, 3233 (1976).
[8] M. H. Kalos, J. K. Percus and M. Rao, J. Stat. Phys. **17**, 111 (1977).
[9] I. Z. Fisher, *Statistical Theory of Liquids* (University of Chicago, Chicago, 1964).
[10] F. P. Buff, R. A. Lovett, and F. H. Stillinger, Phys. Rev. Lett. **15**, 621 (1965); H. T. Davis, J. Chem. Phys. **67**, 3636 (1977); **70**, 600 (1979).
[11] M. S. Wertheim, J. Chem. Phys. **65**, 2377 (1976).
[12] D. G. Triezenberg and R. Zwanzig, Phys. Rev. Lett. **28**, 1183 (1972).